ASIAN JOURNAL OF CIVIL ENGINEERING (BHRC) VOL. 17, NO. 4(2016)
PAGES 495-513

OPTIMAL STRUCTURAL WEIGHT FOR FLEXIBLE-BASE BUILDINGS UNDER STRONG GROUND MOTION EXCITATIONS

B. Ganjavi*
Department of Civil Engineering, University of Mazandaran, Babolsar, Iran

Received: 27 August 2015; **Accepted:** 3 November 2015

ABSTRACT

In this paper, an optimization methodology proposed for the achievement of optimal (minimum) structural weight for flexible-base shear buildings under earthquake excitation. The underlying soil is considered as a homogeneous half-space which is replaced by a simplified 3-DOF system, based on the concept of Cone Models. Through intensive nonlinear dynamic analyses of buildings with consideration of soil-structure interaction (SSI) effect subjected to a group of artificial earthquakes, and using uniform distribution of inter-story ductility demand over the height of structures, an optimization procedure for seismic design of inelastic shear-buildings incorporating SSI effects is developed to achieve minimum structural weight. It is shown that the seismic performance of such a structure is superior to those designed by code-compliant seismic load pattern such that the optimized structures experience significantly less structural weight as compared with those designed based on ASCE/SEI 7-10 load pattern.

Keywords: Soil-structure interaction; optimal design; inelastic behaviour; seismic code; optimal structural weight.

1. INTRODUCTION

In force-based design procedure the distribution of story stiffness and strength along the height of the structures are designed primarily based on the static forces that are mainly based on elastic structural behaviour analyses of fixed-base structures under seismic lateral forces and account for inelastic behaviour in a somewhat indirect manner. The height-wise distribution of these lateral load patterns from various standards such as EuroCode 8 [1], Mexico City Building Code [2], Uniform Building Code [3], ASCE/SEI 7-10 [4], and International Building Code, IBC 2012 [5] depends on the fundamental period of the structures and their mass. They are derived primarily based on elastic dynamic analysis of

*E-mail address of the corresponding author: b.ganjavi@umz.ac.ir (B. Ganjavi)

the corresponding fixed-base structures without considering soil-structure interaction (SSI) effect. The seismic lateral load patterns in all aforementioned provisions are based on the assumption that the soil beneath the foundation is rigid, and hence the influence of SSI effect on load lateral pattern is not taken into account. The adequacy of using the code-specified lateral load patterns for fixed-base building structures have been investigated during the past two decades [6-12]. Recently, several studies have been conducted by researchers to evaluate and improve the code-specified design lateral load patterns based on the inelastic behavior of the structures [10, 12-15]. However, all studies have been concentrated on the different types of structures with rigid foundation, i.e., without considering SSI effects. Recent studies have demonstrated that SSI can significantly affect the seismic responses of structures located on soft soils by changing the overall stiffness and energy dissipation mechanism of the systems [16-23]. In fact, a soil-structure system behaves as a different system having longer period and generally higher damping due to energy dissipation by hysteretic behavior and wave radiation in the soil.

More recently, several studies have been conducted by researchers to improve the code-specified design lateral load patterns based on the inelastic behavior of the structures [8-10, 12-15]. They proposed new lateral load patterns for various types of fixed-base systems based on different optimization techniques. However, nothing has been performed yet on optimum seismic design of buildings with consideration of SSI effects. For the first time, Ganjavi and Hao (2013) [24] developed a new optimization algorithm for optimum seismic design of "*elastic*" shear-building structures with SSI effects. The adopted method has been based on the concept of uniform deformation distribution proposed by Moghadam and Hajirasouliha (2006) [10] for fixed-base shear building structures. Based on numerous optimum load patterns derived from numerical simulations and nonlinear statistical regression analyses, a new load pattern for elastic soil-structure systems with shallow foundation has been proposed. They showed that using the proposed load pattern could lead to a more uniform distribution of deformations over the height of structures. The designed structures also experience up to 40% less structural weight as compared with the code-compliant or aforementioned optimum patterns proposed for fixed-base structures [24].

In the present study, by performing intensive numerical simulations of responses of inelastic soil-structure shear buildings with various dynamic characteristics and SSI parameters an optimization methodology proposed for the achievement of minimum structural weight for flexible-base buildings under earthquake excitation.

2. SOIL-STRUCTURE MODELING AND GROUND MOTIONS

The studied superstructure model is based on the structural modeling explained by FEMA 440 (2005) [25], in which, in some cases engineers can simplify complex structural models into MDOF shear-building models which are called stick models. The well-known shear-beam model which is one of the most frequently used models that facilitate performing a comprehensive parametric study is utilized here as superstructure model [12, 21, 22, 24, 26]. In the MDOF shear-building models utilized in the present study, each floor is assumed as a lumped mass to be connected by elasto-plastic springs. Story heights are 3.2 m and total

structural mass is considered as uniformly distributed along the height of the structure. A bilinear elasto-plastic model with 2% strain hardening in the force-displacement relationship is used to represent the hysteretic response of story lateral stiffness. In all MDOF models, lateral story stiffness is assumed as proportional to story shear strength distributed over the height of the structure. Five percent Rayleigh damping is assigned to the first mode and the mode in which the cumulative mass participation is at least 95%. In this investigation, an ensemble of 15 synthetic earthquake ground motions with different characteristics is compiled. All the selected ground motions are obtained from earthquakes with magnitude greater than 6 having closest distance to fault rupture more than 15 km without pulse type characteristics. The selected ground motions are components of six earthquakes including Imperial Valley 1979, Morgan Hill 1984, Superstition Hills 1987, Loma Prieta 1989, Northridge 1994 and Kobe 1995, and have shear wave velocity ranging from 90 to 350 m/s. To be consistent, using SeismoMatch software [27] these seismic ground motions are adjusted to the elastic design response spectrum of IBC-2012 with soil type *E*.

Using the sub-structure method, the soil can be modeled separately and then combined to establish the soil-structure system. The soil-foundation element is modeled by an equivalent linear discrete model based on the cone model with frequency-dependent coefficients and equivalent linear model [28]. The foundation is considered as a circular rigid disk and the flexibility of the foundation is not taken into account. Cone model based on the one-dimensional wave propagation theory represents circular rigid foundation with mass m_f and mass moment of inertia I_f resting on a homogeneous half-space. In lieu of the rigorous elasto-dynamical approach, the simplified cone model can be used with sufficient accuracy in engineering practice [29]. The foundation mass, m_f, is assumed such that foundation uplift does not occur due to the design earthquake load according to ASCE7-10 [4]. Only the inertial part of the SSI is considered in this study i.e., the kinematic interaction effect is not included assuming that the rigid foundation lies on the surface of the soil with no embedment and is undergone to vertically incident plane shear with particle motion in the horizontal direction. Typical shear-building models of fixed-base and flexible-base systems used in this study are shown in Figure 1. The sway (h) and rocking (φ) degrees of freedom are defined as representatives of translational and rocking motions of the shallow foundation, respectively, disregarding the slight effect of vertical and torsional motion. The stiffness and energy dissipation of the supporting soil are represented by springs and dashpot, respectively. In addition, soil material damping is assumed as commonly used viscous damping so that more intricacies in time-domain analysis are avoided. To consider the frequency-dependent rotational spring and dashpot coefficients, the additional internal rotational degree of freedom, θ, can be assigned to a polar mass moment of inertia, m_θ, and connected to the foundation mass with zero-length element using a rotational dashpot. Also, to modify the effect of soil incompressibility, an additional mass moment of inertia ΔM_φ can be added to the foundation for υ greater than 0.33 [28]. In this case the dilatational shear wave velocity, V_p is limited to $2V_s$ [29]. The coefficients of springs and dashpots for sway and rocking used to define the soil-shallow foundation model are summarized as follows:

$$k_h = \frac{8\rho V_s^2 r}{2-\upsilon}, \qquad c_h = \rho V_s A_0 , \qquad k_\varphi = \frac{8\rho V_s^2 r^3}{3(1-\upsilon)}, \qquad c_\varphi = \rho V_p I_0 \tag{1}$$

$$m_\theta = \frac{9\pi\rho r^5}{128}(1-\upsilon)\left(\frac{V_p}{V_s}\right)^2, \qquad \Delta M_\varphi = 0.3\pi(\upsilon - 1/3)\rho r^5 \tag{2}$$

where k_h, c_h, k_φ and c_φ are sway stiffness, sway viscous damping, rocking stiffness, and rocking viscous damping, respectively. Equivalent radius and area of cylindrical foundation are denoted by r and A_0. Besides, ρ, υ, V_p and V_s are respectively the specific mass density, Poisson's ratio, dilatational and shear wave velocity of soil. To consider the soil material damping, ζ_0, in the soil-foundation element, each spring and dashpot is respectively augmented with an additional parallel connected dashpot and mass.

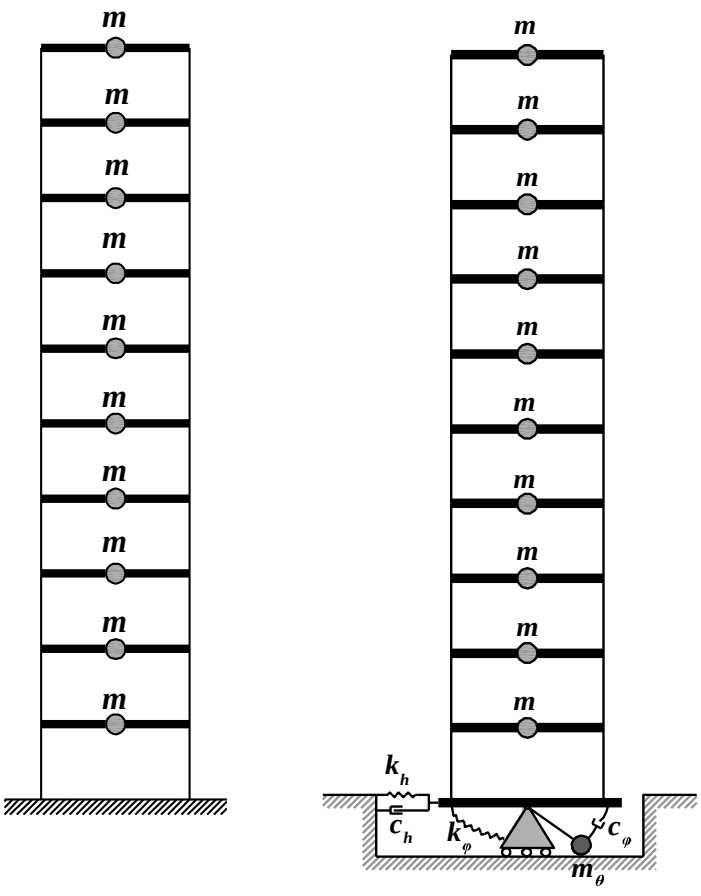

Figure 1. Typical shear-building models (a) fixed-base model and (b) flexible-base model

3. GOVERNING INTERACTING PARAMETERS

The response of the soil-structure system essentially depends on the size of structure, dynamic characteristics of the soil and structure, the soil profile as well as the applied excitation. It has been shown that the effect of these factors can be best described by two parameters of the non-dimensional frequency and aspect ratio [30]. To consider soil flexibility in a given system, the non-dimensional frequency, $a_0 = (\omega_{fix}\bar{H})/V_s$ a_0 , is defined as an index for the structure-to-soil stiffness ratio, where ω_{fix} and $\bar{H}$ denote the circular frequency of the fixed-base structure and the effective height of the superstructure, respectively. Stewart et al. (1999) [31] proposed that the most important parameter controlling the significance of inertial SSI is $\bar{H}/(T_{fix}V_s)$, and that the effects of inertial SSI are not generally important for small values of $\bar{H}/(T_{fix}V_s)$. Not that if this parameter is multiplied by 2π, the a_0 parameter defined above will be obtained. It can be shown that the practical range of a_0 for conventional building structures is from zero for the fixed-base structure to about 3 for the case with severe SSI effect [32]. Besides, $\bar{H}$ is the effective height of structure corresponding to the fundamental mode properties of the MDOF building. Aspect ratio of the building is defined as $\bar{H}/r$. Other parameters to conduct a parametric study for soil-structure systems can be defined as follows: Inter-story displacement ductility demand of the structure is defined as $\mu = D_m/D_y$, where D_m and D_y are the maximum inter-story displacement demand resulted from a specific earthquake ground motion excitation and the yield inter-story displacement corresponds to the structural stiffness of the same story, respectively. Structure-to-soil mass ratio is defined as $\bar{m} = m_{tot}/\rho r^2 H$, where H is total height of the structure. Foundation-to-structure mass ratio m_f/m_{tot}. In the present study, the foundation mass ratio is assumed to be equal to the story mass of the MDOF buildings. As mentioned above, the first two factors, i.e., a_0 and $\bar{H}$, affecting the responses more prominently are usually considered as the governing parameters which define the main SSI effect. μ controls the inelastic behavior of the structure. The other parameters, having less significance, may be set to some typical values for conventional buildings [28, 33]. In this study, The Poisson's ratio is considered to be 0.4 for the alluvium soil and 0.45 for the soft soil. Also, a damping ratio of 5% is assigned to the soil material.

4. ASCE-7-10 SEISMIC DESIGN LATERAL LOADING PATTERN FOR FIXED-BASE BUILDINGS

The general formula of the lateral load pattern specified by the aforementioned seismic codes is defined as:

$$F_i = \frac{w_i h_i^k}{\sum_{j=1}^{n} w_j h_j^k} . V_b \tag{3}$$

where F_x and V_b are respectively the lateral load at level *i* and the total design lateral force (Base shear); w_j and w_i are the portion of the total gravity load of the structure located at the level *j* or *i*; h_j and h_i are the height from the base to the level *j* or *i; n* is the number of stories; and *k* is an exponent that differs from one seismic code to another. In IBC-2012 [5] and ASCE/SEI 7-10 [4], *k* is related to fundamental period of the structure, which is equal to 1 or 2 for structures having a period of 0.5 sec or less, and for structures having a period of 2.5 sec or more, respectively. For structures having a period between 0.5 and 2.5 sec, *k* is computed by linear interpolation between 1 and 2.5. Note that when *k* is equal to 1, the pattern corresponds to an inverted triangular lateral load distribution and the response of building, thus, is assumed to be controlled primarily by the first mode. While *k* equal to 2 corresponds to a parabolic lateral load pattern with its vertex at the base in which the response is assumed to be influenced by higher mode effects.

5. OPTIMIZATION ALGORITHM FOR THE ACHIEVEMENT OF MINIMUM STRUCTURAL WEIGHT

In this section, the optimization algorithm adopted by Ganjavi and Hao (2013) [24] for optimum elastic shear-strength distribution of soil-structure systems is modified to take into account for the inelastic behaviour of structures. In this approach, the structural properties are modified so that inefficient material is gradually shifted from strong to weak parts of the structure. This process is continued until a state of uniform deformation is achieved. In the present study, the seismic demand parameters used to quantify the structural damage and optimization criterion are the inter-story displacement ductility ratio (μ) and structural weight. The following step-by-step optimization algorithm is proposed for shear-building soil-structure systems to estimate the optimum inelastic lateral force distribution corresponding to the "*minimum structural weight*":

1. Select number of stories for MDOF soil-structure building and assign an arbitrary value for total stiffness and strength and then distribute them along the height of the structure based on the arbitrary lateral load pattern, e.g., uniform or triangular patterns. It will be noted that the lateral story stiffness is assumed as proportional to the story shear strength distributed over the height of the structure.
2. Select an earthquake ground motion.
3. Select key parameters for SSI effects including aspect ratio, $\bar{H}/r$, and non-dimensional frequency, a_0.
4. Consider the fundamental period of fixed-base structure and scale the total stiffness without altering the stiffness distribution pattern such that the structure has a specified target fundamental period.

5. Select a target ductility ratio and Perform dynamic analysis for the soil-structure system subjected to the selected ground motion and compute the total shear strength demand, $(V_{bs})_i$. If the computed ductility ratio is equal to the target value within the 1% of the accuracy, no iteration is necessary. Otherwise, total base shear strength is scaled (by either increasing or decreasing) until the target ductility ratio is achieved. To do this the following equation originally is proposed:

$$(V_{bs})_{i+1} = (V_{bs})_i \left(\frac{\mu_{\max}}{\mu_t}\right)^{\beta} \tag{4}$$

where $(V_{bs})_i$ is the total base shear strength of MDOF system at *i*th iteration; μ_t and $\mu_{\max}$ are respectively the target ductility ratio and maximum story ductility ratio among all stories. Parameter β is an iteration power which is more than zero. Results of this study show that for Inelastic state ($\mu_t > 1$) β value, depending on the fundamental period, can be approximately defined as $\beta = 0.05 - 0.1$ for $T_{fix} \le 0.5$ and $\beta = 0.1 - 0.25$ for $0.5 < T_{fix} < 1.5$ and $\beta = 0.25 - 0.4$ for $T_{fix} > 1.5$.

6. Calculate the coefficient of variation (COV) of story ductility distribution along the height of the structure and compare it with the target value of interest which is considered here 0.02. If the value of COV is less than the presumed target value, the current structural weight is regarded as minimum weight. Otherwise, the story shear strength and stiffness patterns are scaled until the COV decreases below or equal to the target value.
7. Stories in which the ductility demand is less than the presumed target value are identified and their shear strength and stiffness are reduced. To obtain the fast convergence in numerical computations, the equations proposed by Hajirasouliha and Moghaddam (2009) [12] and Ganjavi and Hao (2013) [24] for respectively fixed-base systems and elastic soil-structure systems are modified for inelastic soil-structure systems as follows:

$$[S_i]_{q+1} = [S_i]_q . \left[\frac{\mu_i}{\mu_t}\right]^{\alpha} \tag{5}$$

where $[S_i]_q$ = shear strength of the *i*th floor at *q*th iteration, μ_i =story ductility ratio of the *i*th floor and α = convergence parameter that has been considered equal to 0.1- 0.2 as the acceptable range by Hajirasouliha and Moghaddam (2009) [12] for elastic and inelastic fixed-base structures. Based on intensive analyses performed in the present study for soil-structure systems in inelastic range of response, it is concluded that opposed to elastic state very lower values of α need to be utilized for convergence problem in inelastic response in comparison with those of elastic one. Results of this study show a constant value may not guaranty achieving the fastest convergence for all cases of soil-structure systems. Based on intensive nonlinear dynamic analyses on inelastic shear-building structures in which the Rayleigh-type damping is used for the damping modelling, α= 0.07 for $\mu_t \le 3$ and α= 0.1 for $\mu_t > 3$ are approximately proposed for convergence problem of soil-structure systems in

inelastic response. Now, a new pattern for lateral strength and stiffness distributions is obtained.

8. Control the current maximum story ductility ratio ($\mu_{\max}$) and refine the total base shear strength of soil-structure systems if $\mu_{\max}$ is not equal to the target value within the 1% of the accuracy. Otherwise, go to the next step.
9. Control the current fixed-base period and modify it if it is not equal to the target value within the 1% of the accuracy. Otherwise, control the current Rayleigh-type damping coefficients and modify them if they are not equal to the previous values within the 1% tolerance. Otherwise, go to the next step.
10. Convert the optimum shear strength pattern to the optimum lateral force pattern corresponding "*minimum structural weight"*.
11. Repeat steps 1–10 for different number of stories, earthquake ground motions, key parameters ($\bar{H}/r$ and a_0), target periods and target ductility ratio.

6. EFFICIENCY OF THE PROPOSED OPTIMIZATION TECHNIQUE

To show the efficiency of the proposed method to achieve optimum weight for soil-structure systems in inelastic range of response the above algorithm is applied to the 10- and 20-story buildings with T_{fix} = 1.5 sec, μ= 4, 8, $\bar{H}/r$ = 3, and $a_0 = 3$ subjected to 15 simulated earthquakes. Figure 2 illustrates a comparison of the average height-wise distribution of story ductility demand resulted from utilizing three load patterns including (1) ASCE/SEI 7-10 [4] (2) optimum patterns of fixed-base and (3) optimum patterns of soil-structure systems. As seen, there is a significant difference between the optimum pattern of soil-structure systems and the other two patterns. It can be seen that while using the SSI optimum pattern results in a completely uniform distribution of the deformation, using both the ASCE/SEI 7-10 and fixed-base optimum patterns lead to a very non-uniform distribution of ductility demand along the height of the soil-structure systems in inelastic range of vibration. The efficiency of the proposed optimization procedure can be investigated by calculating the coefficient of variation (COV) of story ductility demand distribution along the height of structures. The COV is a statistical measure of the dispersion of data points, here ductility demand ratio along the building height. It is defined as the ratio of the ductility demand standard deviation to the mean ductility among all stories. For instance, based on the results presented in Fig. 2, the average COV values of story ductility demand distributions resulted from applying ASCE/SEI 7-10 [4] pattern, the fixed-base optimum pattern and SSI optimum pattern (proposed SSI) are respectively 44%, 54.7% and 0.4%, for 10-story building with μ= 8. The corresponding values are also 39%, 62.5% and 0.5%, for 20-story building with μ= 8. This indicates that SSI phenomenon through changing the dynamic characteristics of structures can more significantly affect damage distribution along the height of structures in inelastic range of response when compared to that of the elastic state. As a result, utilizing fixed-base optimum load pattern may not result in an optimum seismic performance of soil-structure systems and, thus, a more adequate load pattern accounting for both SSI effects and inelastic behaviour should be defined and proposed for

soil-structure system.

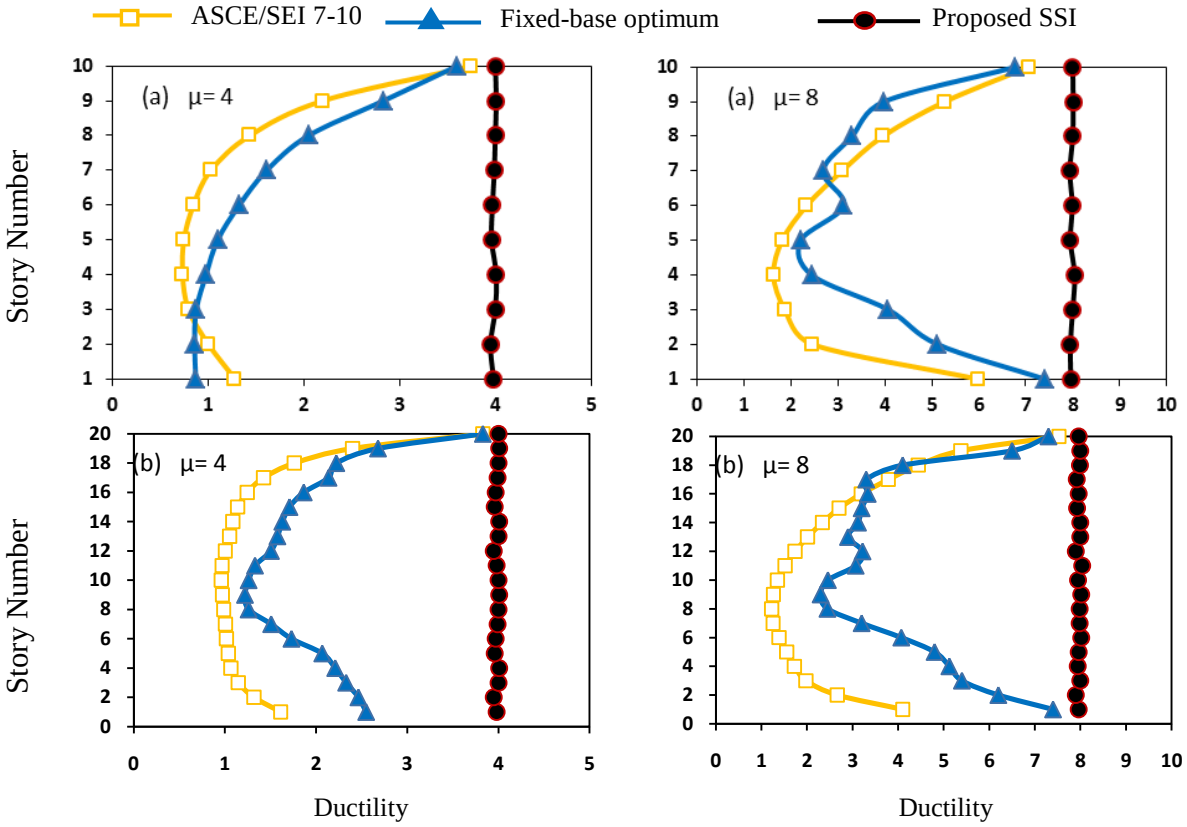

Figure 2. Mean story ductility patterns obtained from 15 earthquakes for buildings that were designed based on ASCE-7-10, fixed-base optimum patterns and proposed optimization algorithm for SSI systems (T_{fix} = 1.5 sec, $\bar{H}/r$ =3, a_0 =3), (a): 10 stories and (b): 20 stories

The efficiency of the proposed optimum load pattern can also be investigated by comparing the structural weight index resulted from a given load pattern (here ASCE/SEI 7-10 [4]) with that of the optimum load pattern corresponding to a given earthquake ground motion. In this study, structural weight index for a specific structure with given fundamental period, target ductility demand, non-dimensional frequency and aspect ratios is regarded as the seismic structural weight normalized by PGA and total structural mass. The loading pattern that corresponds to the "*minimum weight index*" is considered as the most adequate loading pattern i.e., optimum pattern [12, 24].

Figure 3 shows the mean percentage of structural weight reduction of optimum structures with respect to those designed based on ASCE/SEI 7-10 [4] for the 10-story soil-structure systems with low (μ= 2) and high (μ= 6) level of nonlinearity and $\bar{H}/r$ =3. It is clearly seen that even for the case of less SSI effect (a_0 =1) the optimum structures experience up to 56%

less structural weight as compared with the structures designed based on ASCE/SEI 7-10 [4] lateral load pattern. The efficiency of the optimum patterns will be more pronounced for the structures with longer periods in which higher mode effect is predominant.

In another point of view, as mentioned above, the COV of ductility demand distribution along the building height could be used for assessing the efficiency of design load patterns. This is because the more uniform the ductility demand distribution, the better is the seismic performance of the structure. To this end, mean spectra of COV for different soil-stricture systems with 20 stories and with two levels of inelasticity designed based on ASCE/SEI 7-10 [4] seismic code and proposed optimum patterns are depicted in

. It is observed that for the structures designed in accordance to ASCE/SEI 7-10 [4] seismic code, increasing the soil flexibility and the ductility demands are generally accompanied by an increase in the mean percentage of COV of inter-story ductility demands. However, nearly for all the optimum structures regardless of the period range, soil flexibility and level of inelastic behavior the mean values of COV are less than 4% meaning uniform damage distribution along the height of structures. This demonstrates the the efficiency of the optimum proposed technique for soil-structure systems.

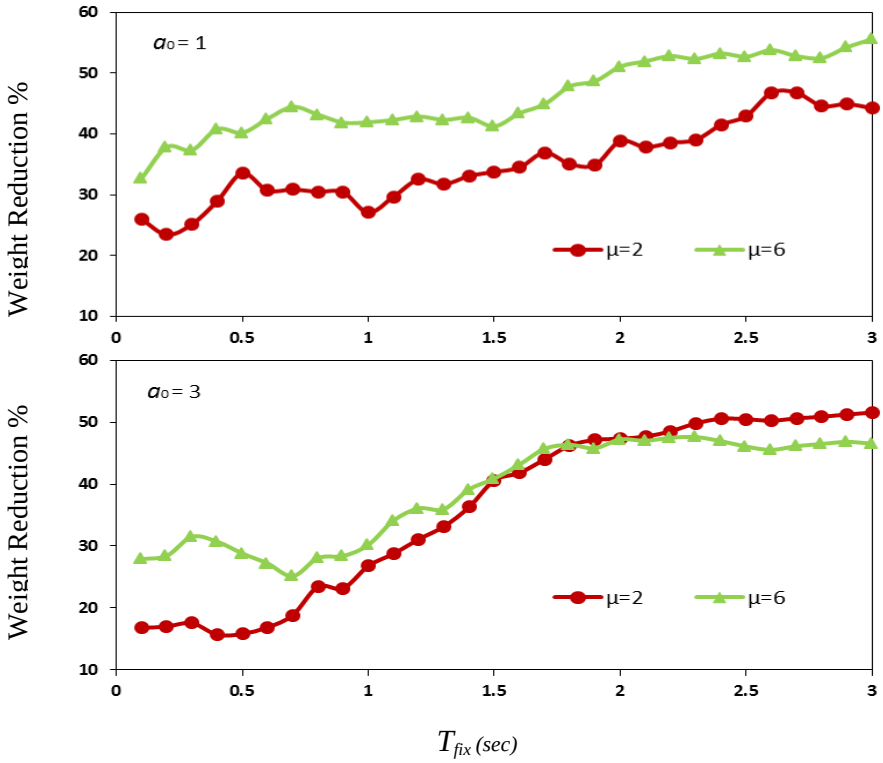

Figure 3. The percentage of structural weight reduction of optimum structures with respect to those designed based on ASCE/SEI 7-10 for the 10-story soil-structure systems; average of 15 earthquakes; $\bar{H}/r$ =3

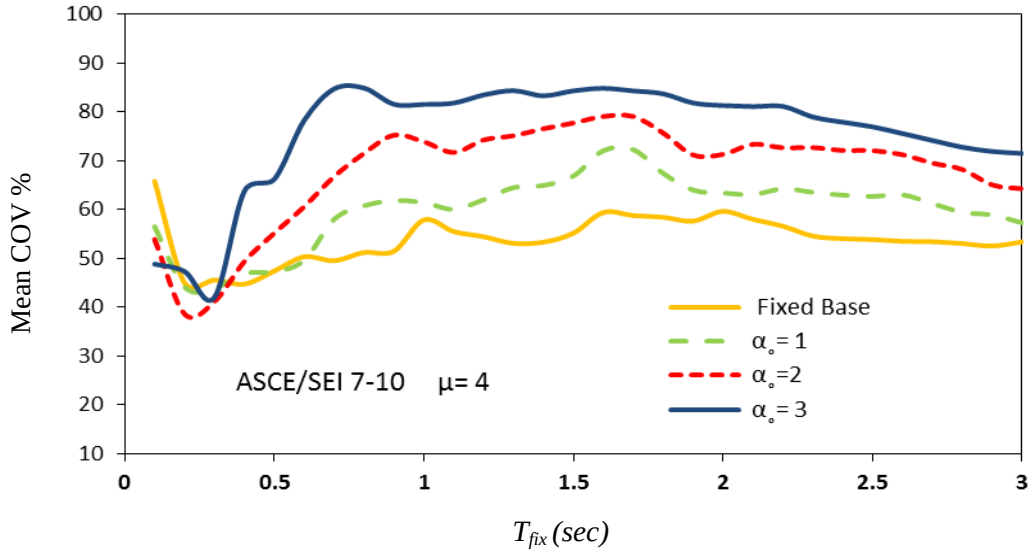

Figure 4. Mean COV% of inelastic fixed- base and soil–structure systems with 20 stories designed according to ASCE/SEI 7-10 load patterns; $\bar{H}/r$ =3

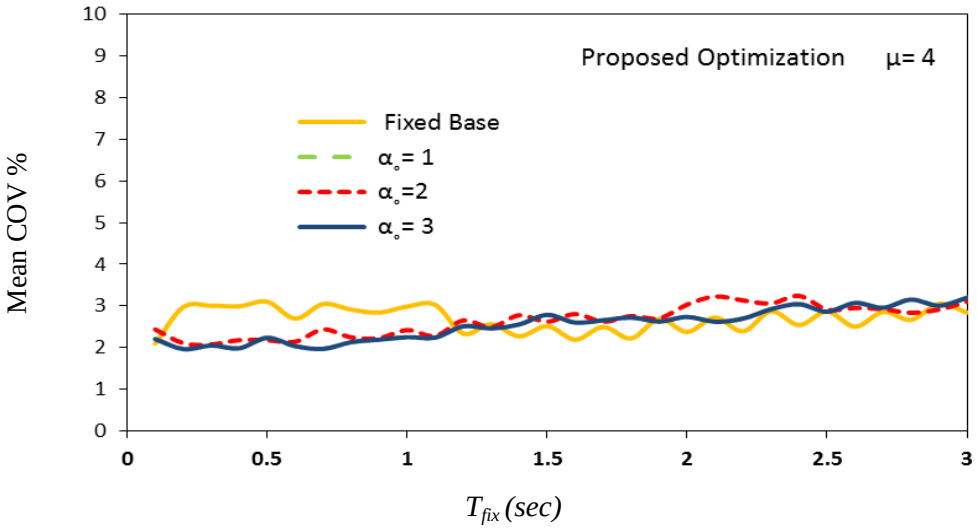

Figure **5.** Mean COV% of inelastic fixed- base and soil–structure systems with 20 stories designed according to proposed optimum algorithm; $\bar{H}/r$ =3.

7. SEISMIC LOAD PATTERN FOR OPTIMUM STRUCTURAL WEIGHT OF SOIL- STRUCTURE SYSTEMS

To generalize the use of the proposed optimization algorithm for seismic design of soil-structure systems, it is necessary to develop statistical models for estimating the optimal design lateral load pattern as a function of relevant structural and soil characteristics. Generally, it is believed that for design purpose, the design earthquake ground motion should be classified for each structural performance and soil type category. More reliable load pattern, then, can be obtained by commuting the mean values of optimum patterns associated to the design earthquakes compatible with each seismic design spectrum. Utilizing the proposed optimization algorithm, nearly 40,000 optimum lateral load patterns considering structural inelastic behaviour are derived for soil-structure systems [34]. For each fundamental period, dimensionless frequency, aspect ratio and ductility demand ratio the mean optimum load pattern corresponding to 21 matched earthquake ground motions are obtained. It is expected that designs based on the mean patterns would exhibit a more uniform damage (ductility demand) and less structural weight along the height of soil-structure systems. Based on the results of the study carried out by the author and nonlinear statistical regression analysis, a new load pattern was proposed to incorporate the effect of inelastic behaviour for soil-structure systems as follows:

$$F_i = a_i + b_i T_{fix}^{\,0.75}.\, Ln(T_{fix}) + c_i\, e^{(-0.9T_{fix})} \tag{6}$$

where F_i = optimum load component at the *i*th story; T_{fix} = fixed-base fundamental period; and a_i , b_i and c_i = constant coefficients of *i*th story which are functions of aspect ratio ($\bar{H}/r$), dimensionless frequency (a_0) and inter-story ductility demand (μ) that can be obtained in reference [34] for each level (relative height) of structure. As an instance, these constant coefficient for μ= 4 are provided in Tables 1 and 2. The adequacy of the proposed load pattern to achieve optimum structural weight for soil-structure systems will be investigated in the next section.

Table 1: Constant coefficients of Eq. (6) as function of relative height (μ= 4)

a_0 = 1	$\bar{H}/r$ = 1			$\bar{H}/r$ = 3			$\bar{H}/r$ = 5		
Relative Height	a_i	b_i	c_i	a_i	b_i	c_i	a_i	b_i	c_i
0.05	34.58	16.48	23.34	27.66	22.04	32.03	22.29	25.69	38.79
0.10	31.59	13.70	26.23	26.94	16.14	30.51	23.52	18.26	33.32
0.20	29.49	7.69	26.52	25.93	8.46	28.81	22.66	9.16	31.25
0.30	28.62	4.28	26.46	25.18	3.79	27.93	22.60	3.30	29.34
0.40	28.74	1.43	24.89	26.58	0.01	24.89	27.70	-2.45	20.78
0.50	32.40	-2.01	19.10	32.51	-4.47	16.31	33.53	-6.99	12.90
0.60	41.26	-6.91	5.44	40.61	-7.57	6.01	41.86	-9.66	3.98
0.70	53.47	-10.17	-11.13	53.59	-10.56	-9.49	55.03	-11.79	-10.82
0.80	66.76	-9.63	-25.45	69.98	-10.36	-26.91	72.42	-10.27	-27.52
0.90	85.31	-6.69	-43.21	91.09	-5.26	-45.22	91.89	-3.04	-41.44
1.00	133.12	5.90	-80.06	143.14	6.05	-89.06	144.81	10.38	-87.37

Table 2: Constant coefficients of Eq. (6) as function of relative height (μ= 4)

a_0 = 3	$\bar{H}/r$ = 1			$\bar{H}/r$ = 3			$\bar{H}/r$ = 5		
Relative Height	a_i	b_i	c_i	a_i	b_i	c_i	a_i	b_i	c_i
0.05	43.95	24.15	17.84	54.14	35.58	-7.15	83.83	32.70	-56.30
0.10	38.78	18.66	21.89	34.50	31.80	18.86	57.41	31.28	-20.98
0.20	34.69	9.15	22.29	14.09	21.79	44.55	17.88	27.43	34.45
0.30	32.28	3.74	22.72	11.02	8.18	44.98	3.80	13.49	52.56
0.40	33.27	-1.34	18.71	19.75	-5.08	29.46	4.80	-6.62	46.04
0.50	35.86	-5.47	13.65	31.37	-12.37	13.92	14.49	-14.80	35.45
0.60	40.38	-8.89	6.84	41.21	-15.80	4.28	29.69	-16.94	20.60
0.70	48.30	-11.64	-3.87	51.44	-13.83	-2.48	48.69	-14.98	3.75
0.80	59.61	-11.44	-17.21	68.95	-12.88	-18.92	72.82	-14.14	-19.71
0.90	78.46	-6.27	-36.74	97.39	-9.71	-47.97	102.44	-9.35	-46.82
1.00	126.75	8.70	-82.37	159.51	0.91	-115.0	176.30	-4.07	-128.67

8. ADEQUACY OF PROPOSED OPTIMUM LATERAL LOAD PATTERN FOR SOIL-STRUCTURE SYSTEMS

The adequacy of the proposed load pattern (Eq.6) and ASCE/SEI 7-10 pattern [4] are investigated in this section for soil-structural systems through comparing the structural weight index which is related to the economy of the seismic resistant system. For this purpose, the values of weight index of the 10-story shear buildings designed based on the two patterns (i.e., proposed and ASCE/SEI 7-10 [4] patterns) for 28 fundamental periods ranging from 0.3 to 3 sec, two values of ductility demand, μ= 2 and 6, two values of aspect ratio ($\bar{H}/r$ =1, 3) and two values of dimensionless frequency (a_0 =1, 3) are calculated subjected to 20 matched earthquake ground motions. Then, the ratio of mean (average) values of weight index (R_{WI}) associated to the two aforementioned patterns to those related to the optimum pattern are computed and illustrated in Figs. 5 and 6. Based on the results presented in these figures, it can be observed that for all ranges of period, nonlinearity and SSI effect, the load pattern proposed in this study gives superior results when compared to those of ASCE/SEI 7-10 [4] load patterns. The superiority is more pronounced for the cases of longer periods. As seen, the ratios of required to the optimum structural weight index for models designed with Eq. 6 are, on average, from 1.03 to 1.25 which can be considered as near optimum for practical purposes. Except for the cases of short periods with sever SSI effect and low level of nonlinearity, the efficiency of the code-compliant load pattern (ASCE/SEI 7-10 [4]) significantly diminishes. As an example, for the cases of average slenderness ratio with severe SSI effect with T_{fix} = 2 sec, the values of structural weight for structures designed with load patterns of ASCE/SEI 7-10 [4] and Eq.6 (this study) are respectively 89.9% and 11.2% above the optimum weight in low inelastic response and 89.5% and 12.5% above the optimum weight in high inelastic response. This implies that significant improvement is achieved by utilizing the proposed load pattern of this study for soil-structure systems with inelastic behavior.

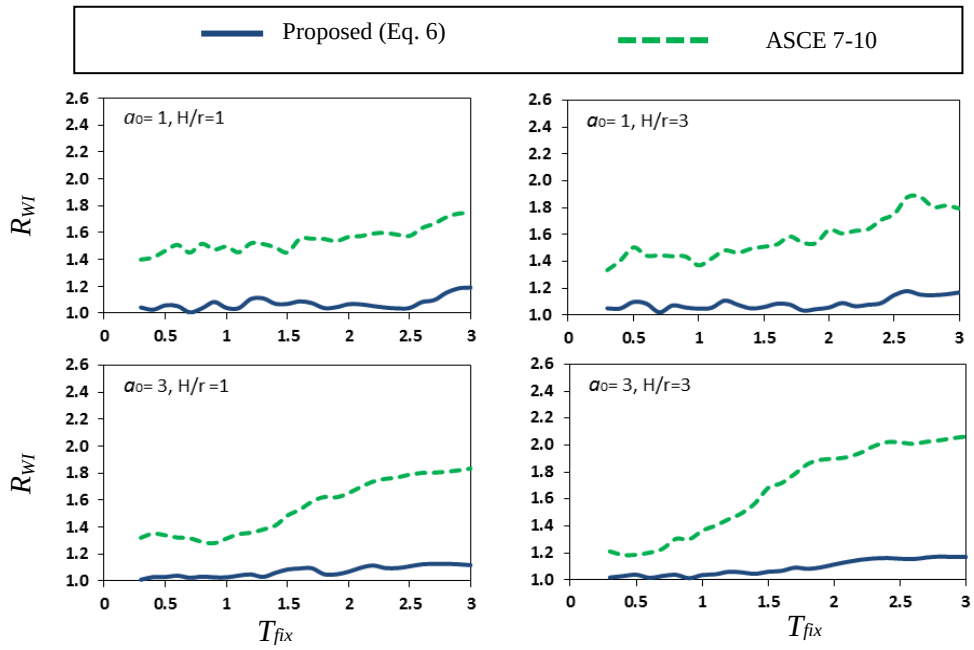

Figure 5. The spectra of ratio of required to optimum weight for the 10-story SSI systems designed according to proposed and ASCE 7-10 patterns; average of 15 earthquakes (μ= 2)

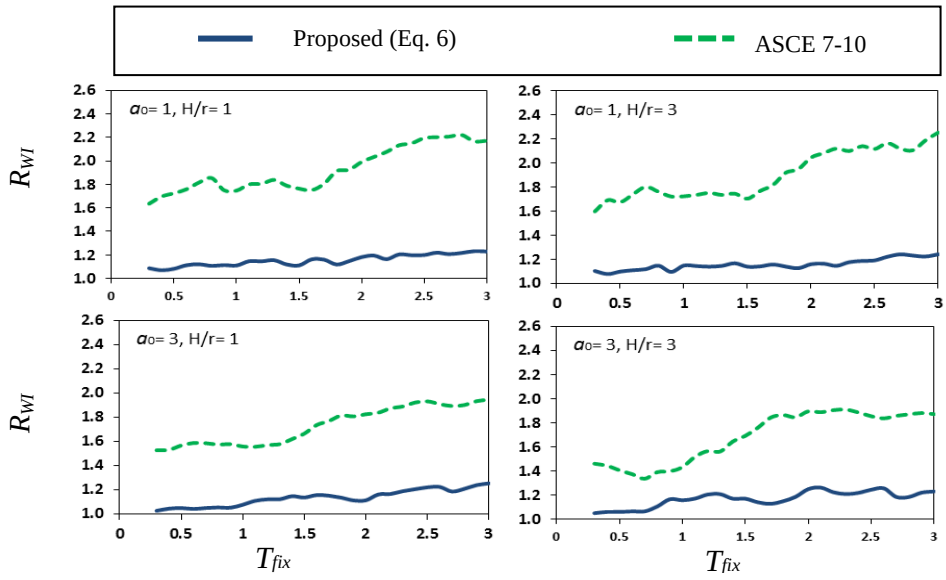

Figure 6. The spectra of ratio of required to optimum weight for the 10-story SSI systems designed according to proposed and ASCE 7-10 load patterns; average of 15 earthquakes (μ= 6)

9. CONCLUSIONS

An optimization methodology has been proposed for the achievement of minimum structural weight for flexible-base buildings under earthquake excitation taken into consideration of

SSI effects. Based on intensive numerical analyses of structural models with different structural and foundation conditions subjected to 21 earthquake ground motions, a new optimum load pattern has been proposed for structural design with consideration of SSI effect and structural inelastic behaviour. The efficiency of the proposed optimization algorithm were investigated by comparing the structural weight index and COV resulted from ASCE/SEI 7-10 [4] with those of the optimum load pattern corresponding to a given earthquake ground motion. It was concluded that even for the case of less SSI effect the optimum structures experience signaficantly less structural weight as compared with the structures designed based on ASCE/SEI 7-10 [4] lateral load pattern. The efficiency of the optimum patterns will be more pronounced for the structures with longer periods in which higher mode effect is predominant. Based on the results presented in this study, it was observed that for all ranges of period, nonlinearity and SSI effects, the load pattern proposed in this study generally gives superior results when compared to those of ASCE/SEI 7-10 [4] load patterns. The superiority is more pronounced for the cases of longer periods. More research works for more complex structural configurations and behaviour are deemed necessary for developing a practical methodology applicable to design and analysis of structures to earthquake ground motions.

REFERENCES

1. CEN. EuroCode 8: Final draft of EuroCode 8: Design of structure for earthquake resistance – Part 1: General rules for buildings, Bruxelles, European Committee for Standardization, 2003.
2. Mexico City Building Code, 2003.
3. UBC97. Uniform building code. International Conference of Building Officials Whittier CA, 1997.
4. ASCE/SEI 7-10. Minimum Design Loads for Buildings and Other Structures, American Society of Civil Engineers, Reston VA, 2010.
5. IBC-2012. International Building Code. ICC Birmingham AL, 2012.
6. Anderson JC, Miranda E, Bertero VV. Evaluation of the seismic performance of a thirty-story RC building. UCB/EERC-91/16. Earthquake Engineering Research Center, University of California, Berkeley, 1991.
7. Gilmore TA, Bertero VV. Seismic performance of a 30-story building located on soft soil and designed according to UBC 1991. UCB/EERC-93/04, Earthquake Engineering Research Center, niversity of California, Berkeley, 1993.
8. Leelataviwat S, Goel SC, Stojadinovic B. Toward performance-based seismic design of structures, *Earthquake Spectra*, No. 3, **15**(1999) 435-61.
9. Mohammadi RK, El Naggar M, Moghaddam H. Optimum strength distribution for seismic resistant shear buildings, *International Journal of Solids and Structures*, No. 22, **41**(2004) 6597-12.
10. Moghaddam H, Hajirasouliha I. Toward more rational criteria for determination of design earthquake forces, *International Journal of Solids and Structures*, No. 9, **43**(2006) 2631-45.

11. Ganjavi B, Vaseghi Amiri J, Ghodrati Amiri G, Yahyazadeh Ahmadi Q. Distribution of drift, hysteretic energy and damage in reinforced concrete buildings with uniform strength ratio, *The 14th World Conference on Earthquake Engineering*, Beijing, China, October, 2008.
12. Hajirasouliha I, Moghaddam H. New lateral force distribution for seismic design of structures, *Journal of Structural Engineering*, No. 8, **135**(2009) 906-15.
13. Park K, Medina RA. Conceptual seismic design of regular frames based on the concept of uniform damage, *Journal of Structural Engineering*, No. 7, **133**(2007) 945-55.
14. Goel SC, Liao WC, Reza Bayat M, Chao SH. Performance-based plastic design (PBPD) method for earthquake-resistant structures: an overview, T*he Structural Design of Tall and Special Buildings*, Nos. 1-2, **19**(2010) 115-37.
15. Hajirasouliha I, Asadi P, Pilakoutas K. An efficient performance-based seismic design method for reinforced concrete frames, *Earthquake Engineering & Structural Dynamics*, No. 4, **41**(2012) 663-79.
16. Wang JF, Lin CC. Seismic performance of multiple tuned mass dampers for soil – irregular building interaction systems, *International Journal of Solids and Structures*, No. 20, **42**(2005) 5536-54.
17. Barcena A, Esteva L. Influence of dynamic soil–structure interaction on the nonlinear response and seismic reliability of multistorey systems, *Earthquake Engineering & Structural Dynamics*, No. 3, **6**(2007) 327-46.
18. Tang Y, Zhang J. Probabilistic seismic demand analysis of a slender RC shear wall considering soil–structure interaction effects, *Engineering Structures*, No. 1, **33**(2011) 218-29.
19. Raychowdhury P. Seismic response of low-rise steel moment-resisting frame (SMRF) buildings incorporating nonlinear soil–structure interaction (SSI), *Engineering Structures*, No. 3, **33**(2011) 958-67.
20. Aviles J, Eduardo Pérez-Rocha L. Use of global ductility for design of structure - foundation systems, *Soil Dynamics and Earthquake Engineering*, **31**(2011) 1018-26.
21. Khoshnoudian F, Ahmadi E. Effects of pulse period of near-field ground motions on the seismic demands of soil–MDOF structure systems using mathematical pulse models, *Earthquake Engineering & Structural Dynamics*, No. 11, **42**(2013) 1565-82.
22. Abedi-Nik F, Khoshnoudian F. Evaluation of ground motion scaling methods in soil – structure interaction analysis, *The Structural Design of Tall and Special Buildings*, No. 1, **23**(2014) 54-66.
23. Ghannad MA, Jafarieh AH. Inelastic displacement ratios for soil–structure systems allowed to uplift, *Earthquake Engineering & Structural Dynamics*, No. 9, **43**(2014) 1401-21.
24. Ganjavi B, Hao H. Optimum lateral load pattern for seismic design of elastic shear-buildings incorporating soil - structure interaction effects, *Earthquake Engineering & Structural Dynamics*, No. 6, **42**(2013) 913-33.
25. FEMA 440. Improvement of nonlinear static seismic analysis procedures, Federal Emergency Management Agency prepared by Applied Technology Council, 2005.
26. Ganjavi B, Hao H. Strength reduction factor for MDOF soil–structure systems, *The Structural Design of Tall and Special Buildings*, No. 3, **23**(2014) 161-80.

27. Seism Soft Seismo Match, A computer program for adjusting earthquake records to match a specific target response spectrum, 2011.
28. Wolf JP. Foundation Vibration Analysis using Simple Physical Models ed.), Prentice-Hall, Englewood Cliffs, NJ, 1994.
29. Wolf JP, Deeks, AJ. Foundation Vibration Analysis: A Strength-of-Materials Approach ed.), Elsevier, Burlington, MA, 2004.
30. Veletsos AS. Dynamics of structure-foundation systems, Structural and Geotechnical Mechanics, (1977) 333-61.
31. Stewart JP, Seed RB, Fenves GL. Seismic soil-structure interaction in buildings. II: Empirical findings, *Journal of Geotechnical and Geoenvironmental Engineering*, No. 1, **125**(1999) 38-48.
32. Ghannad MA, Jahankhah H. Site-dependent strength reduction factors for soil-structure systems, *Soil Dynamics and Earthquake Engineering*, **27**(2007) 99-110.
33. Veletsos AS, Meek JW. Dynamic behaviour of building-foundation systems, *Earthquake Engineering & Structural Dynamics*, **3**(1974) 121-38.
34. Ganjavi B. A Parametric Study on the Effect of Soil-Structure Interaction on Seismic Response of MDOF and Equivalent SDOF System, Phd Thesis, The University of Western Australia, 2012.